END-TO-END BEAM SIMULATIONS FOR THE NEW MUON G-2 EXPERIMENT AT FERMILAB

M. Korostelev*, I. R. Bailey, Lancaster University and the Cockcroft Institute, UK
A. Herrod, A. Wolski, University of Liverpool and the Cockcroft Institute, UK
W. Morse[1], J. Morgan[2], D. Stratakis[1,2], V. Tishchenko[1]
[1]Brookhaven National Laboratory, Upton NY, USA
[2]Fermi National Accelerator Laboratory, Batavia IL, USA

Abstract

The aim of the new muon g-2 experiment at Fermilab is to measure the anomalous magnetic moment of the muon with an unprecedented uncertainty of 140 ppb. A beam of positive muons required for the experiment is created by pion decay. Detailed studies of the beam dynamics and spin polarization of the muons are important to predict systematic uncertainties in the experiment. In this paper, we present the results of beam simulations and spin tracking from the pion production target to the muon storage ring. The end-to-end beam simulations are developed in Bmad and include the processes of particle decay, collimation (with accurate representation of all apertures) and spin tracking.

INTRODUCTION

The muon has a magnetic dipole moment related to its spin by $\vec{\mu}_s = g(e\hbar/2m)\vec{s}$. Radiative corrections from quantum electrodynamics lead to some small difference from $g = 2$ expected from the Dirac equation. The difference is measured by the anomalous magnetic moment $a_\mu = \left(\frac{g-2}{2}\right)$, which is a fundamental constant relating the magnetic moment and the spin. Precise experimental determination of the anomalous magnetic moment of the muon (muon anomaly) has the potential to reveal the effects of particle physics beyond the Standard Model.

The new muon g-2 experiment at Fermilab (E989) [1] will measure the muon anomaly to an uncertainty of 140 ppb. A beam of longitudinally polarized muons with "magic" momentum $p_m = 3.094$ GeV/c will be injected into the storage ring and circulated in a highly uniform magnetic field. In this case, the difference in angular frequency between the precession of muon spin and the muon momentum is given by simple formula: $\omega_a = -\frac{e}{m}a_\mu B$. The muon anomaly a_μ can be determined by measuring two quantities: the storage ring magnetic field B using a number of NMR probes, and the angular frequency ω_a using 24 calorimeters distributed inside the ring. The beam of positive muons decays into positrons and neutrinos. Due to the chiral nature of the weak force, the highest energy positrons are strongly correlated with the direction of muon spin. Tuning the calorimeters to register only high energy positrons, the number of positrons detected (time spectrum) is modulated by the angular frequency ω_a as the spin precesses.

The key improvement of the new muon g-2 measurement is that the Fermilab accelerator facility can provide a high intensity, pure muon beam to increase the statistics for the g-2 experiment.

PARTICLE TRACKING

A high intensity 8 GeV proton beam coming from the booster hits the production target and produces a beam of secondary particles that is a mixture of different species, but consists mainly of protons and positive pions. At the end of the M2M3 beamline (length 300 m) that connects the target and delivery ring, most of the pions have decayed into positive muons. The mixed beam enters the delivery ring (circumference 505 m) and circulates several turns to achieve a longitudinal separation between the protons and muons, due to the velocity difference between the different species. On the fourth turn, the longitudinal separation is sufficient for a fast kicker to remove cleanly the trailing proton beam. Then, on the same turn, the muons are extracted into the M4M5 beam line (length 140 m) that transfers them to the storage ring entrance. A more detailed description of the lattice can be found in Ref. [1].

The existing accelerator facility at Fermilab is being adapted to the requirements of the g-2 experiment. The baseline lattice design is now established, though some optimization may still be done. Accurate tracking simulations are needed to evaluate the lattice performance.

A beamline model (corresponding to the baseline design) from the production target to the entrance of the storage ring (including the delivery ring) has been developed in Bmad [2]. Modelling the lattice in Bmad allows the implementation of particle tracking, collimation, pion decay and spin tracking. A special module has been developed in F90 to include pion decay kinematics in the Bmad tracking.

The apertures of all the quadrupole and dipole magnets were carefully included in the Bmad model according to the latest engineering specification. The Bmad implementation makes it possible to assign an accurate description for the "star chamber" aperture into quadrupoles (without any approximation). The majority of quadrupoles in both beamlines and the delivery ring have the star chamber aperture.

The 6D distribution of secondary particles at the exit of

* maxim.korostelev@cockcroft.ac.uk

the production target was obtained from MARS simulation of 10^9 protons on the target, and was used as the initial distribution in the tracking simulations. The initial numbers of secondary particles per proton on target (POT) are as follows: 12.45×10^{-3} protons, 1.17×10^{-3} positive pions and 3.04×10^{-6} positive muons. The longitudinal distribution of all particles was assumed to follow that of the incident proton beam.

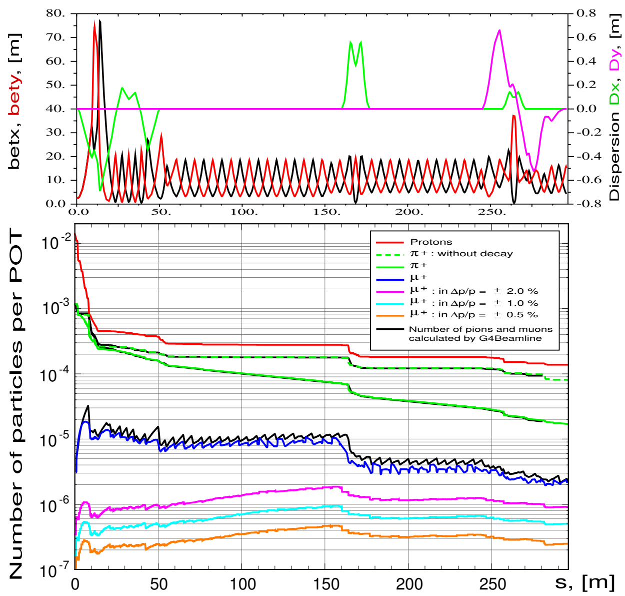

Figure 1: Optics functions (top plot) and number of particles per POT (bottom plot) along the M2M3 beamline, showing protons (red line), pions (green line), pions (with pion decay turned off, green dashed line), muons (blue line). Muons with momentum in the range of $\pm 2\%$, $\pm 1\%$ and $\pm 0.5\%$ with respect to 3.094 GeV/c are shown by magenta, light blue and orange lines, respectively. Black lines correspond to results from an independent calculation using G4Beamline.

Figure 1 shows the population of protons, pions and muons as a function of position along the M2M3 beamline, found from the Bmad tracking. Secondary particles at the target have a wide momentum distribution. The separation magnet located after the production target selects particles with momentum around 3.1 GeV/c, which decreases significantly the number of pions at the beginning of the beamline. Although the pion decay angle (the angle between the initial direction of the muon and its parent pion) does not exceed 14.5 mrad, the transverse phase-space of all the created muons is 112 mm.mrad (calculated from the second-order moments), which is larger than the beamline acceptance of 40 mm.mrad. This causes a loss of muons in the FODO straight sections because of collimation on the quadrupole apertures where the betatron functions have local maxima. In the lab frame, the momentum of the created muon can differ from the momentum of the parent pion by a factor from 0.57 to 1.0 with uniform probability. Thus, the average momentum of all created muons is 0.67 GeV/c less than the average momentum of all the decayed pions, as shown in Fig. 2. Moreover, the momentum spread of the created muons is larger than the momentum spread of the decayed pions. This leads to a significant loss of muons with momentum outside $\pm 2\%$ from the magic momentum in the achromatic bend (around $s = 160$ m) where horizontal dispersion occurs. At the end of the M2M3 beamline the muon momentum distribution is centered on 3.1 GeV with one standard deviation of $\pm 2.7\%$.

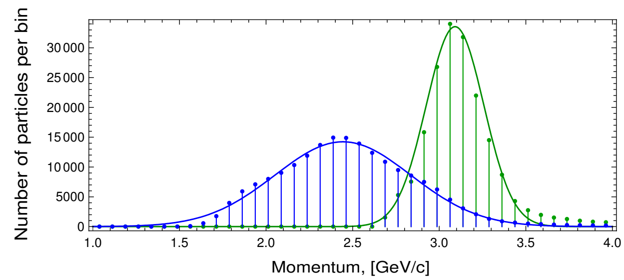

Figure 2: Momentum distribution of all created muons (blue line) and all decayed pions (green line). Muons: the average momentum is 2.43 GeV/c with one standard deviation of 0.4 GeV/c. Pions: the average momentum is 3.093 GeV/c with one standard deviation of 0.17 GeV/c.

The results of pion tracking performed using G4Beamline [3] are shown as a black line in Fig. 1. There is a good agreement between the two different codes regarding the numbers of pions and muons.

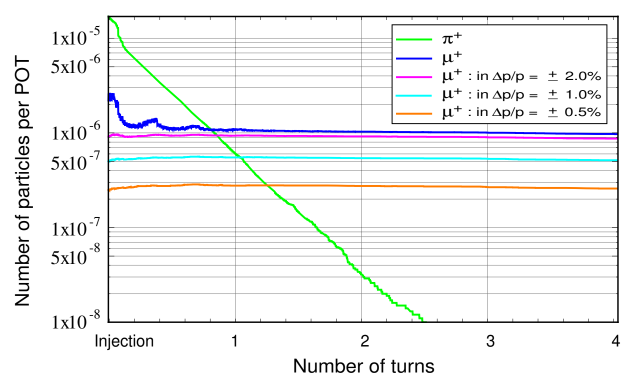

Figure 3: Number of particles as a function of turn number in the delivery ring.

Approximately half of the muons injected into the delivery ring are lost in the first turn because of the momentum acceptance of the ring, as shown in Fig. 3. The population of muons does not decrease significantly on subsequent turns. All the pions have decayed before the third turn.

The M4M5 beamline transfers to the storage ring inflector approximately 80% of muons extracted from the delivery ring, as shown in Fig. 4. Muon loss takes place mainly in the vertical dogleg and in the final focus of the beamline. The momentum distribution of muons entering the

ISBN 978-3-95450-147-2

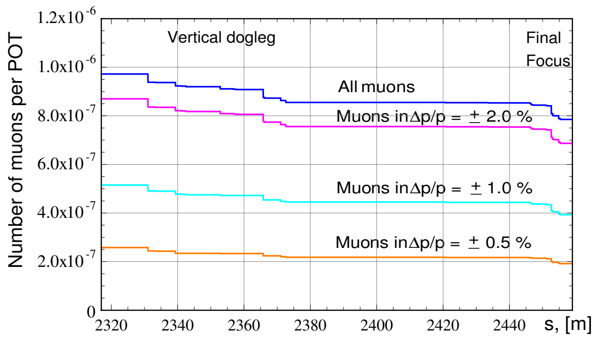

Figure 4: Number of muons along M4M5 beamline.

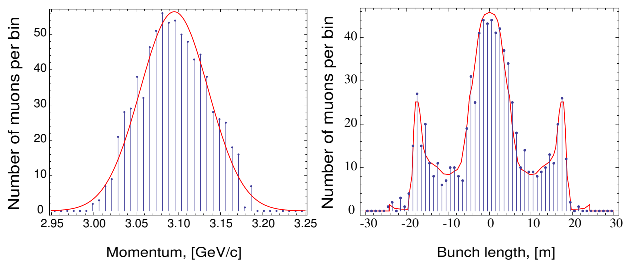

Figure 5: Momentum distribution (left plot) and longitudinal distribution (right plot) of muons at the end of M4M5 beamline. The red line on the right-hand plot shows the initial distribution of pions at the target normalized to the number of muons.

inflector is shown in Fig. 5 (left plot). The muons have average momentum 3.095 GeV/c with one standard deviation of 1.3%. Figure 5 (right plot) shows that the final longitudinal distribution of the muon beam does not vary from the initial longitudinal distribution of the pions. The total number of muons per POT is 7.8×10^{-7} where 6.9×10^{-7}, 3.9×10^{-7} and 1.9×10^{-7} muons per POT are within the range of momentum $\pm2\%$, $\pm1\%$ and $\pm0.5\%$, respectively. The horizontal and vertical emittance of the muon beam calculated from the second-order moments is 10 mm.mrad.

The direction of the muon spin is opposite to the muon momentum after pion decay. The change in angle between the spin and momentum over a number of turns N in a storage ring is $\Delta\phi_a = 2\pi N\gamma a_\mu$, that is 0.214 rad per revolution for muons with magic momentum p_m. Therefore, the difference in precession angles for off-momentum muons is $d\phi_a/d\delta = 2\pi N\gamma a_\mu = 0.214N$ rad where $\delta = (p-p_m)/p_m$. Figure 6 (left plot) shows the distribution of spin precession angles at the inflector entrance after four turns in the delivery ring found from spin tracking. The spin polarization is directed 0.851 rad from the beam direction with one standard deviation of 0.0157 rad. The vertical spin component has an average value of 10^{-4} rad with standard deviation 0.004 rad, as shown in Fig. 6 (right plot).

The correlation between the spin precession angle and the momentum is show in Fig. 7. The linear fit to the tracking data obtained at extraction from the delivery ring and at the exit of M4M5 beamline is $\phi_a = (0.852\delta + 0.87)$ rad

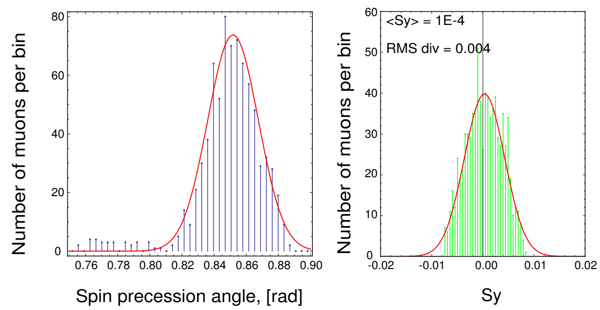

Figure 6: Distribution of spin precession angles and vertical spin components at the end of M4M5 beamline.

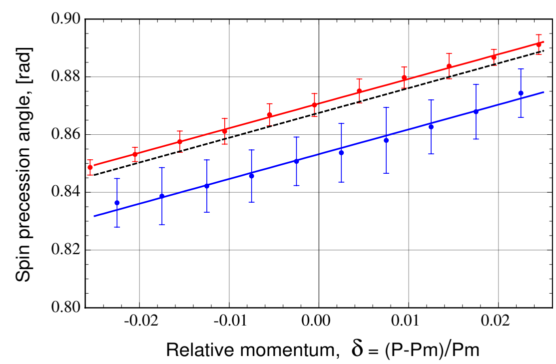

Figure 7: Correlation between angle of spin precession and momentum at extraction from delivery ring (red line) and at the exit from the M4M5 beamline (blue line). The error bars show ± one standard deviation of the spread in spin angles from the average value (points). The dashed line shows the correlation between precession angle and momentum predicted by theory.

and $\phi_a = (0.857\delta + 0.853)$ rad, respectively. Taking into account the fact that the average precession angle of muons entering the delivery ring is 0.0084 rad (because of the bend achromat), the results of the spin tracking are in good agreement with the analytical estimate $\phi_a = (0.859\delta + 0.867)$ rad, shown in Fig. 7 as a dashed line.

CONCLUSIONS

Beamline models from the pion production target to the entrance to the storage ring have been established in Bmad, including accurate descriptions of the apertures, tracking of particles with decay processes, collimation, and spin dynamics. There is good agreement between the results from Bmad and from an independent model in G4Beamline. Studies of muon spin dynamics show the expected behaviour in terms of the polarization angle and spin precession rate for particles with non-zero energy deviation. Some work is still needed to include a 3D field map of the inflector in the Bmad model. Development of a model of the storage ring in Bmad is in progress to investigate the systematic uncertainties in the differential decay distributions.

REFERENCES

[1] J. Grange *et al.*, “Muon (g-2) Technical Design Report,” arXiv:1501.06858, (2015).

[2] www.lepp.cornell.edu/∼dcs/bmad/

[3] D. Stratakis *et al.*, “Performance Analysis for the New g-2 Experiment,” these proceedings (IPAC’16).

ISBN 978-3-95450-147-2